Inorg. Chem. **2007**, *46*, 8291–8301

Cadmium(II) Complexes of (Arylazo)imidazoles: Synthesis, Structure, Photochromism, and Density Functional Theory Calculation

K. K. Sarker,[†] D. Sardar,[†] K. Suwa,[‡] J. Otsuki,[‡] and C. Sinha*[,†]

Department of Chemistry, Inorganic Chemistry Section, Jadavpur University, Kolkata 7000 032, India, and Department of Materials and Applied Chemistry, College of Science and Technology, Nihon University, 1-8-4 Kanda Surugadai, Chiyoda-ku, Tokyo 101-8308, Japan

Received June 20, 2007

Reaction between CdX_2 and 1-alkyl-2-(phenylazo)imidazole (RaaiR′) has isolated complexes of composition $Cd(RaaiR')_2X_2$ in MeOH or MeCN. Crystallization of $Cd(RaaiR')_2I_2$ from *N*,*N*-dimethylformamide (DMF) has separated $[Cd(RaaiR')I_2 \cdot DMF]$, while $Cd(RaaiR')_2X_2$ (X = Cl and Br) remains unchanged in its composition upon crystallization under identical conditions. The structure has been established by spectral (UV–vis and ^1H NMR) data and confirmation in the latter case by a single-crystal X-ray diffraction study of $[Cd(TaiMe)I_2 \cdot DMF]$ [where TaiMe = 1-methyl-2-(*p*-tolylazo)imidazole]. UV-light irradiation in a MeCN solution of $Cd(RaaiR')_2I_2$ and $[Cd(RaaiR')I_2 \cdot DMF]$ shows trans-to-cis isomerization of coordinated azoimidazole. The reverse transformation, cis-to-trans, is very slow with visible light irradiation. Quantum yields ($\phi_{t\rightarrow c}$) of trans-to-cis isomerization are calculated, and the free ligand shows higher ϕ values than their cadmium(II) iodo complexes. The cis-to-trans isomerization is a thermally induced process. The activation energy (E_a) of cis-to-trans isomerization is calculated by a controlled-temperature experiment. The effects of the anions (Cl^-, Br^-, I^-, and ClO_4^-) and the number of coordinated azoimidazoles (RaaiR′) [Cd(RaaiR′) or $Cd(RaaiR')_2$] on the rate and quantum yields of photochromism are established in this work. A slow rate of photoisomerization of $[Cd(RaaiR')_4](ClO_4)_2$ compared to $Cd(RaaiR')I_2$ or $Cd(RaaiR')_2X_2$ may be associated with the increased mass and rotor volume of the complexes. The rate of isomerization is also dependent on the nature of X and follows the sequence $Cd(RaaiR')_2Cl_2 < Cd(RaaiR')_2Br_2 < Cd(RaaiR')_2I_2$. It may be related to the size and electronegativity of halide, which reduces the effective molar association in the order of I < Br < Cl and hence the rate. *Gaussian 03* calculations of representative complexes and free ligands are used to explain the difference in the rates and quantum yields of photoisomerization.

1. Introduction

Exploration of the material properties of the organic molecules and their metal complexes is of current research interest. The properties can be varied by changing the ligand types, the presence of substituents, and the different carbocyclic and heterocyclic rings and also by using different metal ions. Toward the study of the properties of the complexes, we have been interested in examining the photochromism of azoheterocycles and the effect on metal coordination thereof. Photochromism is a reversible photoinduced transformation between two molecular states whose absorption spectra differ significantly.[1] Incorporation of photochromic molecules into organic or hybrid organic–inorganic materials leads to the development of very effective devices. Azo-conjugated metal complexes exhibit unique properties upon light irradiation in the area of photon-mode high-density information storage photoswitching devices.[2]

(Arylazo)imidazoles constitute an interesting class of heterocyclic azo compounds as a potential switching group in biological applications and in coordination chemistry because imidazole is a ubiquitous and essential group in biology, especially as a metal-coordinating site. This family

* To whom correspondence should be addressed. E-mail: c_r_sinha@yahoo.com. Fax: 91-033-2413-7121.
[†] Jadavpur University.
[‡] Nihon University.

(1) Rau, H. In *Photochromism, Molecules and Systems*; Dürr, H., Bounas-Laurent, H., Eds.; Elsevier: Amsterdam, The Netherlands, 1990; pp 165–192. Nishihara, H. *Bull. Chem. Soc. Jpn.* **2004**, *77*, 407. Tamai, N.; Miyasaka, H. *Chem. Rev.* **2000**, *100*, 1857. Yagai, S.; Karatsu, T.; Kitamura, A. *Chem.—Eur. J.* **2005**, *11*, 4054.
(2) Ire, M. *Chem. Rev.* **2000**, *100*, 1683. Ikeda, T.; Tsutsumi, O. *Science* **1995**, *268*, 1873. Kawata, S.; Kawata, Y. *Chem. Rev.* **2000**, *100*, 1777. Akitasu, T.; Einaga, Y. *Polyhedron* **2007**, *26*, in press.

10.1021/ic7012073 CCC: $37.00
Published on Web 09/07/2007

Scheme 1. Isomerization of (Phenylazo)imidazole

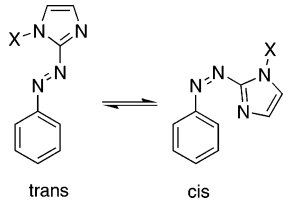

of compounds has been extensively used as ligands for metal ions by us[3−8] and others.[9−11] However, very few reports concerning the photochromic property (Scheme 1) of (arylazo)-imidazole dyes are found in the literature.[12−15] The photochromism of 1-methyl-2-(phenylazo)imidazole (PaiMe)[14] and mercury(II) azoimidazole complexes[15] has inspired us to examine the photochromic property of cadmium(II) complexes of 1-alkyl-2-(arylazo)imidazoles. The influence of halides (Cl^-, Br^-, and I^-), and ClO_4^- on the rates of isomerization and quantum yields will be compared in this report.

2. Results and Discussion

2.1. Synthesis of Complexes. PaiMe (**1a**), 1-methyl-2-(*p*-tolylazo)imidazole (TaiMe, **1b**), 1-ethyl-2-(phenylazo)-imidazole (PaiEt, **2a**), and 1-ethyl-2-(p-tolylazo)imidazole (TaiEt, **2b**) are used in this work to prepare cadmium(II) complexes. The reaction between CdX_2 and the ligand in a MeOH−MeCN (2:1, v/v) mixture has synthesized a coordination complex of composition $[Cd(RaaiR')_2(X)_2]$ [X = Cl (**3** and **4**), Br (**5** and **6**), I (**7** and **8**); RaaiR′ is used as a general abbreviation for 1-alkyl-2-(arylazo)imidazole]. Crystallization of $[Cd(RaaiR')_2(I)_2]$ in MeCN is unsuccessful, and we have tried to crystallize it from a MeCN solution in the presence of *N*,*N*-dimethylformamide (DMF; 1:0.5, v/v). However, the compositions of the crystallized products are different from the previous one and are $[Cd(RaaiR')(I)_2 \cdot DMF]$ (**9** and **10**), while the crystallization of $[Cd(RaaiR')_2(Cl)_2]$ and $[Cd(RaaiR')_2(Br)_2]$ from DMF−MeCN does not change the composition of the complexes. The compounds are nonconducting, and their compositions have been supported by microanalytical data. The reaction of $Cd(ClO_4)_2 \cdot 6H_2O$ and RaaiR′ has separated compounds of composition $[Cd(RaaiR')_4](ClO_4)_2$ (**11** and **12**; Scheme 2). The structures of $[Cd(PaiMe)_2Cl_2]$ (**3a**) and $[Cd(PaiEt)_4](ClO_4)_2$ (**12a**) are reported elsewhere.[16] The complexes **5**−**10** are new and have been established in one case by a single-crystal X-ray diffraction study.

2.2. Spectral Studies. The bands in the Fourier transform infrared (FTIR) spectra of the complexes $[Cd(RaaiR')_2(X)_2]$ (**3**−**8**) and $[Cd(RaaiR')(I)_2 \cdot DMF]$ (**9** and **10**) were assigned upon comparison with the free-ligand data and reported complexes.[16,17] Moderately intense stretchings at 1595−1600 and 1435−1445 cm^{-1} are due to ν(C═N) and ν(N═N), respectively.

The absorption spectra were recorded in a MeCN solution for the new complexes **5**−**10** in 200−900 nm. The characteristics common to the complexes are as follows: (1) a structured absorption band around 370−390 nm with a molar absorption coefficient on the order of 10^4 M^{-1} cm^{-1} and (2) a tail extending into 450 nm. From the analogy with the absorption spectra of PaiMe,[14] it is likely that the large absorption band around 370−390 nm corresponds to $\pi\pi^*$ transitions, while the tail corresponds to a $n\pi^*$ transition. The assignment is also supported by theoretical calculations, as described later. The $\pi\pi^*$ absorption peaks (λ_{max}) for derivatives of (2-phenylazo)imidazole are within the range of 361−375 nm, which is between the $\pi\pi^*$ absorption bands of azobenzene (313 nm) and 4-(*N*,*N*-dimethylamino)azobenzene (390 nm).[18]

The ^1H NMR spectra of $[Cd(RaaiR')_2(X)_2]$ are recorded in CD_3CN, and the signals are assigned (Table 1) unambiguously by spin−spin interaction, by the effect of substitution therein, and on comparison with previously reported data.[15−17,19−21] The atom-numbering pattern is shown in the structure (Scheme 2). Data reveal that the signals in the spectra, in general, are shifted downfield compared with the spectra of the free ligand.[17] The 7,11-H are shifted to higher δ by ∼0.5 ppm. This observation supports the existence of strong interaction between ligands and cadmium(II) in the complexes. Aryl signals are shifted to the lower field side upon Me substitution to the aryl ring. This is due to the electron-donating effect of the Me group. N1−R′ shows the usual signal pattern, as earlier.[17]

2.3. Molecular Structure of $[Cd(TaiMe)I_2(C_3H_7NO)]$. The crystals obtained from the reaction between CdI_2 and TaiMe from a MeOH−MeCN mixture decompose upon

(3) Chand, B.; Ray, U.; Mostafa, G.; Lu. T.-H.; Sinha, C. *J. Coord. Chem.* **2004**, *57*, 627.
(4) Ray, U.; Banerjee, D.; Mostafa, G.; Lu, T.-H.; Sinha, C. *New J. Chem.* **2004**, *28*, 1437.
(5) Dinda, J.; Jasimuddin, S.; Mostafa, G.; Hung, C.-H.; Sinha, C. *Polyhedron* **2004**, *23*, 793.
(6) Jasimuddin, S.; Sinha, C. *Transition Met. Chem.* **2004**, *29*, 566.
(7) Chand, B.; Ray, U.; Mostafa, G.; Cheng, J.; Lu, T.-H.; Sinha, C. *Inorg. Chim. Acta* **2005**, *358*, 1927.
(8) Dinda, J.; Senapoti, S.; Mondal, T.; Jana, A. D.; Chiang, M.; Lu T.-H.; Sinha, C. *Polyhedron* **2006**, *25*, 1125. Mathur, T.; Ray, U. S.; Baruri, B. N.; Sinha, C. *J. Coord. Chem.* **2005**, *58*, 399.
(9) Raj, S. S. S.; Fun, H.-K.; Chen, X.-F.; Zhu, X.-H.; You, X.-Z. *Acta Crystallogr.* **1999**, *C55*, 1644.
(10) Dash, A. C.; Acharya, A.; Sahoo, R. K. *Indian J. Chem.* **1998**, *37A*, 759.
(11) Ackermann, M. N.; Robinson, M. P.; Maher, I. A.; LeBlanc, E. B.; Raz, R. V. *J. Organomet. Chem.* **2003**, *682*, 248.
(12) Endo, M.; Nakayama, K.; Kaida, Y.; Majima, T. *Tetrahedron Lett.* **2003**, *44*, 6903.
(13) Fukuda, N.; Kim, J. Y.; Fukuda, T.; Ushijima, H.; Tamada, K. *Jpn. J. Appl. Phys.* **2006**, *45*, 460.
(14) Otsuki, J.; Suwa, K.; Narutaki, K.; Sinha, C.; Yoshikawa, I.; Araki, K. *J. Phys. Chem. A* **2005**, *109*, 8064.
(15) Sarker, K. K.; Chand, B. G.; Suwa, K.; Cheng, J.; Lu, T.-H.; Otsuki, J.; Sinha, C. *Inorg. Chem.* **2007**, *46*, 670. Otsuki, J.; Suwa, K.; Sarker, K. K.; Sinha, C. *J. Phys. Chem. A* **2007**, *111*, 1403.
(16) Chand, B. G.; Ray, U. S.; Mostafa, G.; Lu, T.-H.; Falvello, L. R.; Soler, T.; Tomas, M.; Sinha, C. *Polyhedron* **2003**, *22*, 3161.
(17) Misra, T. K. Transition Metal Chemistry of 2-arylazoimidazoles: Synthesis, Characterisation and Electrochemical Studies. Ph.D. Thesis, Burdwan University, Burdwan, India, 1999.
(18) Nishimura, N.; Sueyoshi, T.; Yamanaka, H.; Imai, E.; Yamamoto, S.; Hasegawa, S. *Bull. Chem. Soc. Jpn.* **1976**, *49*, 1381.
(19) Misra, T. K.; Das, D.; Sinha, C.; Ghosh, P. K.; Pal, C. K. *Inorg. Chem.* **1998**, *37*, 1672.
(20) Sarker, K. K.; Chand, B. G.; Jana, A. D.; Mostafa, G.; Sinha, C. *Inorg. Chim. Acta* **2005**, *359*, 695.
(21) (a) Chand, B. G.; Ray, U. S.; Cheng, J.; Lu, T.-H.; Sinha, C. *Polyhedron* **2003**, *23*, 1213. (b) Chand, B. G.; Ray, U. S.; Santra, P. K.; Mostafa, G.; Lu, T.-H.; Sinha, C. *Polyhedron* **2003**, *22*, 1205.

Scheme 2. Structures of $Cd(RaaiR')_2(X)_2$ (**3**−**8**), $[Cd(RaaiR')(I)_2 \cdot DMF]$ (**9** and **10**), and $[Cd(RaaiR')_4](ClO_4)_2$ (**11** and **12**)[a]

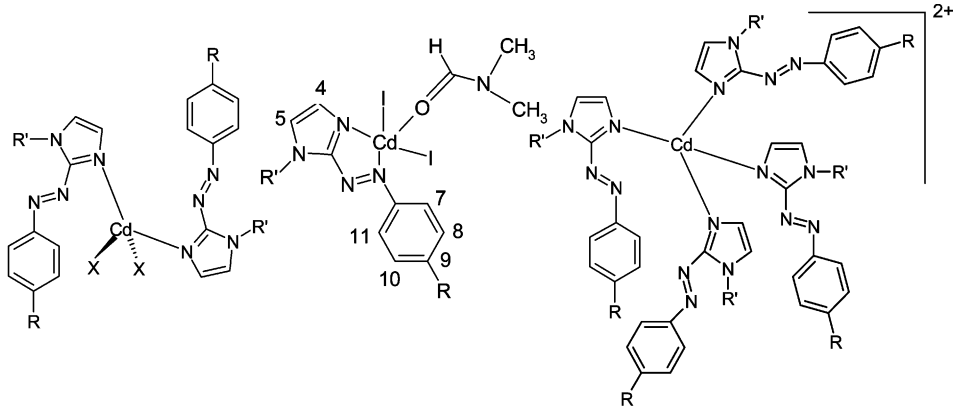

Cd(RaaiR′)$_2$(X)$_2$ (3-8) [Cd(RaaiR′)(I)$_2$.DMF] (9, 10). [Cd(RaaiR′)$_4$](ClO$_4$)$_2$ (11, 12)

[a] $[Cd(PaiMe)_2(Cl)_2]$ (**3a**), $[Cd(TaiMe)_2(Cl)_2]$ (**3b**), $[Cd(PaiEt)_2(Cl)_2]$ (**4a**), $[Cd(TaiEt)_2(Cl)_2]$ (**4b**), $[Cd(PaiMe)_2(Br)_2]$ (**5a**), $[Cd(TaiMe)_2(Br)_2]$ (**5b**), $[Cd(PaiEt)_2(Br)_2]$ (**6a**), $[Cd(TaiEt)(Br)_2]$ (**6b**), $[Cd(PaiMe)_2(I)_2]$ (**7a**), $[Cd(TaiMe)_2(I)_2]$ (**7b**), $[Cd(PaiEt)_2(I)_2]$ (**8a**), $[Cd(TaiEt)_2(I)_2]$ (**8b**), [Cd(PaiMe)(I)$_2$.DMF] (**9a**), [Cd(TaiMe)(I)$_2$.DMF] (**9b**), [Cd(PaiEt)(I)$_2$.DMF] (**10a**), [Cd(TaiEt)(I)$_2$.DMF] (**10b**), $[Cd(PaiMe)_4](ClO_4)_2$ (**11a**), $[Cd(TaiMe)_4](ClO_4)_2$ (**11b**), $[Cd(PaiEt)_4](ClO_4)_2$ (**12a**), and $[Cd(TaiEt)_4](ClO_4)_2$ (**12b**)

Table 1. ^{1}H NMR Spectral Data of $[Cd(RaaR')_2(X)_2]$ [X = Br (**5** and **6**), I (**7** and **8**)] Complexes in $CDCl_3$ at 300 K

	δ (ppm) (J (Hz))							
compd	4-H[a]	5-H[a]	7,11-H[b]	8,10-H[b]	9-R	1- CH_3[e]	1-CH_2	(1-CH_2)CH_3
$Cd(PaiMe)_2(Br)_2$ (**5a**)	7.44	7.34	8.09 (7.0)	7.57[c]	7.57[d]	4.14		
$Cd(TaiMe)_2(Br)_2$ (**5b**)	7.47	7.36	8.00 (7.0)	7.38 (7.0)	2.48[f]	4.13		
$Cd(PaiEt)_2(Br)_2$ (**6a**)	7.46	7.35	8.05 (7.0)	7.50[c]	7.48[d]		4.60[g] (10.0)	1.55[h] (7.5)
$Cd(TaiEt)_2(Br)_2$ (**6b**)	7.41	7.31	8.02 (7.0)	7.32 (7.0)	2.40[c]		4.52[g] (12.0)	1.56[h] (7.5)
$Cd(PaiMe)_2(I)_2$ (**7a**)	7.48	7.38	7.93 (7.0)	7.49[c]	7.49[d]	4.01		
$Cd(TaiMe)_2(I)_2$ (**7b**)	7.42	7.37	8.02 (7.0)	7.37 (7.0)	2.46[f]	4.10		
$Cd(PaiEt)_2(I)_2$ (**8a**)	7.33	7.28	7.65 (7.0)	7.47[c]	7.58[d]		4.24[g] (10.0)	1.32[h] (7.5)
$Cd(TaiEt)_2(I)_2$ (**8b**)	7.33	7.29	8.00 (7.0)	7.35 (7.0)	2.42[c]		4.44[g] (12.0)	1.30[h] (7.5)

[a] Broad singlet. [b] Doublet. [c] Multiplet. [d] δ(9-H). [e] Singlet. [f] δ(9-Me). [g] Quartet. [h] Triplet.

Table 2. Selected Bond Distances (Å) and Angles (deg) for $[Cd(TaiMe)I_2(C_3H_7NO)]$

bond distances (Å)		bond angles (deg)	
Cd−I1	2.7140(12)	I1−Cd−I2	121.15(3)
Cd−I2	2.7306(13)	I1−Cd−N1	115.72(15)
Cd−N1	2.250(5)	I1−Cd−O1	99.6(2)
Cd−N4	2.639(5)	N1−Cd−N4	66.23(17)
Cd−O1	2.380(7)	N1−Cd−O1	83.8(2)
N3−N4	1.264(6)	N4−Cd−O1	149.9(2)
O1−C14	0.986(12)	I2−Cd−N4	102.23(10)
N3−C4	1.399(8)	I1−Cd−N4	91.97(10)
N4−C5	1.421(7)	I2−Cd−N1	122.34(14)
N5−C14	1.252(13)	I2−Cd−O1	95.3(2)

X-ray exposure. Good quality crystals of 1-methyl-2-(phenylazo)imidazolecadmium(II) iodide were grown by slow evaporation of a methanol−DMF (1:0.5, v/v) mixture. The crystal structure of the complex is shown in Figure 1, and the bond parameters are listed in Table 2. The structure shows a distorted trigonal-bipyramidal (TBP) geometry around Cd^{II}. The coordination includes the chelated azoimine Cd−(N=C−N=N−) group [N(azo) is N4 and N(imine) is N1], two Cd−I bonds, and one Cd−O(DMF) bond. The atomic arrangements Cd1, I1, I2, and N1 constitute a trigonal plane, and Cd deviates by ∼0.1 Å from the mean plane. The chelate angle is 66.23(17)° and is comparable with results reported in the series of chelated (arylazo)imidazole complexes of d^{10} metal complexes.[15,16,20,21] The small chelate angle may be the cause for distortion from symmetric TBP geometry. The N4 [N(azo)] and coordinated O (DMF) appear in apexes of the trigonal plane. The Cd−N4 [Cd−N(azo)] bond is the longest [2.639(5) Å] one in the family of M−N(azo) bond lengths so far known in the literature.[15,16,19−23] The elongation may be due to axial coordination of N4 with reference to the trigonal plane described by $CdNI_2$ and from the small chelate bite angle. Although the Cd−N(azo) bond length is very long, it is less than the sum of the van der Waals radii of Cd^{II} (1.58 Å) and N(sp^2) (1.53 Å). This implies significant bonding interaction between these components. The strong coordination of imidazole N to Cd^{II} has significant biochemical implications and explains the strong toxicity of Cd^{II}.[24] Weak and flexible bonds are very effective at inducing some functional properties in the molecules. The weak bonding interaction between Mn^{II} and the N(azo) center in $[Mn(N_3)_2(TaiEt)]_n$ is responsible for structural distortion and, hence, the canting phenomenon and remnant magnetism at low temperature.[22] Because of the long Cd^{II}−N(azo) distance, the molecule may exhibit photophysical activation via cleavage of this bond followed by rotation to introduce photoisomerization. In fact, we have examined the photochromism of these molecules (vide infra). Imidazole and

(22) Ray, U. S.; Ghosh, B. K.; Monfort, M.; Ribas, J.; Mostafa, G.; Lu, T.-H.; Sinha, C. *Eur. J. Inorg. Chem.* **2004**, 250. Bhuina, P.; Ray, U. S.; Mostafa, G.; Ribas, J.; Sinha, C. *Inorg. Chim. Acta* **2006**, *359*, 4660.

(23) Bhunia, P.; Baruri, B.; Ray, U. S.; Sinha, C.; Das, S.; Cheng, J.; Lu, T.-H. *Transition Met. Chem.* **2006**, *31*, 310.

(24) Fergusson, J. E. *The heavy elements: chemistry, environment impact and health effects*; Pergamon: Oxford, U.K., 1990.

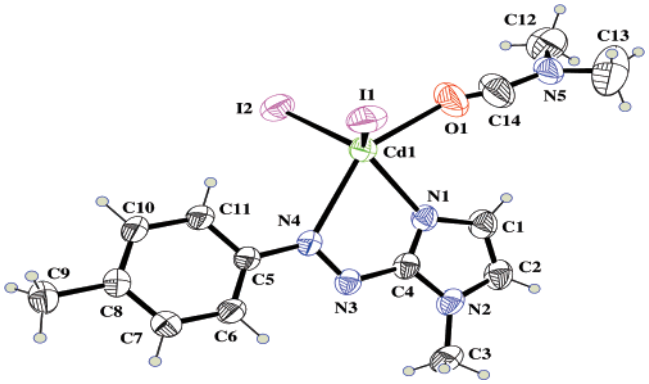

Figure 1. Crystal structure of **9b**.

p-tolyl rings are joined by an azo group, and the dihedral angle is 9.8(3)°. The N═N bond length is 1.264(6) Å and is slightly longer than that of the free ligand [1.250(1) Å].[14,23] The stability of chelated azoimine Cd−(N═C−N═N−) is due to the metal-to-ligand π-back-bonding, and the azo group is directly involved in this process.[17,19] This reduces the M−N(azo) bond length and subsequently increases the N═N bond length from that of the free ligand. The acute chelate angle may develop a strain that is relieved partially by structural distortion and bond-length elongation. The Cd−I distances are comparable with published results.[25]

A $\pi-\pi$ interaction [4.069(4) Å; symmetry, $1-x$, $1-y$, $1-z$] between imidazole and *p*-tolyl rings with the partners of a neighboring molecule has generated a supramolecular motif. The observed weak interactions are C−H---π [3.033 Å, 132.97°, symmetry, $1-x$, $1-y$, $1-z$, where interaction is taking place between C−H (N−CH_3) and the *p*-tolyl ring; 2.882 Å, 148.33°, symmetry, $1-x$, $1-y$, $-z$, where interaction is taking place between DMF C12−H12A and the imidazole ring] and π---π: interactions between imidazole and *p*-tolyl rings of neighboring molecules (4.068 Å, symmetry, $1-x$, $1-y$, $1-z$) and *p*-tolyl---*p*-tolyl (4.226 Å, symmetry, $2-x$, $-y$, $1-z$) have generated a 2D supramolecular sheet (Figure 2).

2.4. Photochromism of [Cd(RaaiR′)$_2$(X)$_2$] and [Cd(RaaiR′)(I)$_2$·DMF] and Comparison with Other Cadmium(II) Azoimidazoles. Upon irradiation of light at λ_{max} to a MeCN solution of the complex, the absorption spectrum changes (Figure 3) in a way similar to that observed for the trans-to-cis isomerization of PaiMe[14,15] and azobenzene.[25] The photochromic observation of a free ligand is shown in Figure 4. The intense peak at λ_{max} decreases, which is accompanied by a slight increase at the tail portion of the spectrum around 490 nm until a stationary state is reached. Subsequent irradiation at the newly appeared longer wavelength peak reverses the course of the reaction, and the original spectrum is recovered up to a point, which is another photostationary state under irradiation at the longer wavelength peak. The quantum yields of the trans-to-cis photoisomerization were determined using those of azobenzene[26] as a standard, and

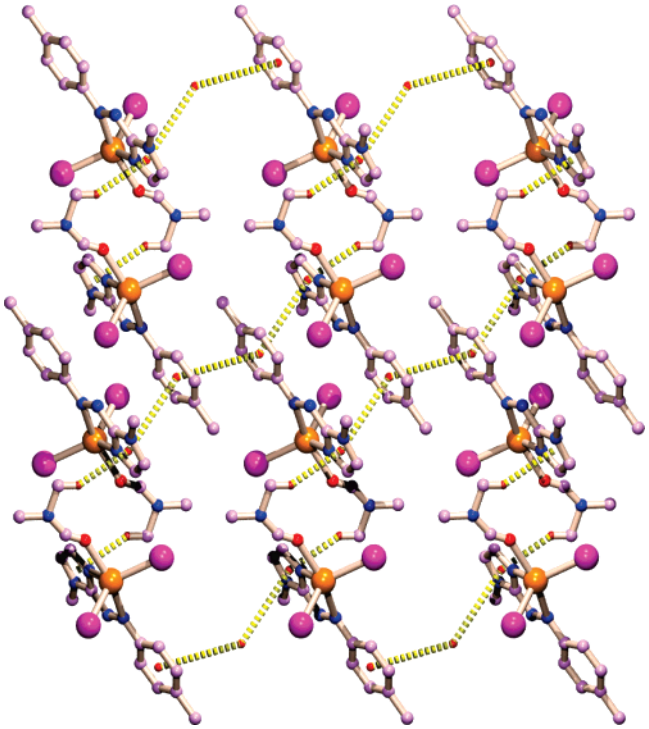

Figure 2. C−H(DMF)---π···$\pi-\pi$·−·π---$\pi-\pi$---π···CH(DMF)−π self-assembly leading to the formation of a 2D supramolecular sheet in the (110) plane.

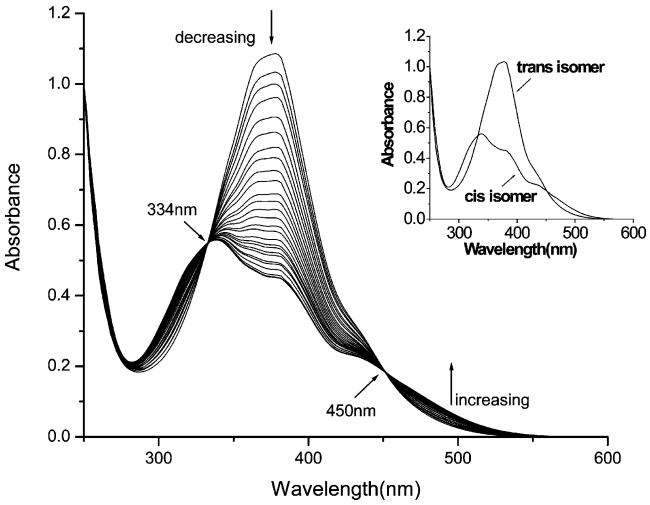

Figure 3. Spectral changes of **7b** in acetonitrile upon repeated irradiation at 380 nm at 3 min intervals at 25 °C. The inset shows spectra of the cis and trans isomers of the compound.

the results are tabulated in Table 3. Thermal cis-to-trans isomerization rates of these (arylazo)imidazoles in MeCN at 298−313 K are collected in Table 4.

The trans-to-cis isomerizations of Cd^{II} complexes of PaiMe, TaiMe, PaiEt, and TaiEt in the presence of different anions Cl^-, Br^-, I^-, and ClO_4^- are carried out in this work. Data are included in Tables 3 and 4 along with photochromic data of PaiMe, TaiMe, PaiEt, and TaiEt. The photoisomerization of the ligand in the complexes is dependent on the nature of the metal ion, its oxidation state, and its structural

(25) Laskar, I. R.; Mostafa, G.; Maji, T. K.; Das, D.; Welch, A. J.; Chaudhuri, N. R. *J. Chem. Soc., Dalton Trans.* **2002**, 1066. Kropidlowska, A.; Chojnacki, J.; Becker, B. *Acta Crystallogr., Sect. C: Cryst. Struct. Commun.* **2006**, *62*, m95.

(26) Zimmerman, G.; Chow, L.; Paik, U. *J. Am. Chem. Soc.* **1958**, *80*, 3528−3531.

Table 3. Excitation Wavelength ($\lambda_{\pi\pi^*}$), Rate of Trans (t) → Cis (c) Conversion, and Quantum Yield ($\phi_{t\rightarrow c}$) in MeCN

compd	$\lambda_{\pi\pi^*}$ (nm)	isosbestic points (nm)	rate of t → c convn × 10^8 (s^{-1})	$\phi_{t\rightarrow c}$
PaiMe (**1a**)	363	333, 431	5.06	0.25 ± 0.03
TaiMe (**1b**)	365	331, 443	3.70	0.218 ± 0.007
PaiEt (**2a**)	364	333, 434	4.83	0.241 ± 0.012
TaiEt (**2b**)	365	328, 444	4.59	0.206 ± 0.006
$Cd(PaiMe)_2Cl_2$ (**3a**)	381	338, 447	2.3810	0.121 ± 0.001
$Cd(TaiMe)_2Cl_2$ (**3b**)	382	331, 447	1.8950	0.093 ± 0.002
$Cd(PaiEt)_2Cl_2$ (**4a**)	375	338, 451	2.0135	0.106 ± 0.003
$Cd(TaiEt)_2Cl_2$ (**4b**)	383	336, 459	1.7125	0.089 ± 0.004
$Cd(PaiMe)_2Br_2$ (**5a**)	383	335, 449	2.6972	0.134 ± 0.002
$Cd(TaiMe)_2Br_2$ (**5b**)	381	334, 451	2.1899	0.109 ± 0.003
$Cd(PaiEt)_2Br_2$ (**6a**)	377	338, 445	2.4721	0.116 ± 0.005
$Cd(TaiEt)_2Br_2$ (**6b**)	388	340, 463	1.7019	0.096 ± 0.006
$Cd(PaiMe)_2I_2$ (**7a**)	375	334, 450	2.8560	0.142 ± 0.004
$Cd(TaiMe)_2I_2$ (**7b**)	380	333, 451	2.5271	0.127 ± 0.002
$Cd(PaiEt)_2I_2$ (**8a**)	373	332, 452	2.5045	0.121 ± 0.001
$Cd(TaiEt)_2I_2$ (**8b**)	390	339, 463	1.9844	0.112 ± 0.001
Cd(PaiMe)I_2·DMF (**9a**)	385	337, 453	3.4330	0.167 ± 0.002
Cd(TaiMe)I_2·DMF (**9b**)	393	339, 465	3.0521	0.158 ± 0.003
Cd(PaiEt)I_2.DMF (**10a**)	382	338, 459	2.9625	0.143 ± 0.002
Cd(TaiEt)I_2.DMF (**10b**)	391	336, 463	2.3967	0.139 ± 0.003
$[Cd(PaiMe)_4](ClO_4)_2$ (**11a**)	382	338, 462	2.1159	0.103 ± 0.004
$[Cd(TaiMe)_4](ClO_4)_2$ (**11b**)	380	331, 468	1.002	0.049 ± 0.001
$[Cd(PaiEt)_4](ClO_4)_2$ (**12a**)	381	335, 458	1.8361	0.089 ± 0.002
$[Cd(TaiEt)_4](ClO_4)_2$ (**12b**)	380	334, 463	0.8052	0.043 ± 0.003

state.[27] The chelate complexes of these metal ions are structurally known.[15,18−20] It is observed that upon irradiation with UV light trans-to-cis photoisomerization proceeded and the cis molar ratio reaches >95%. The absorption spectra of the trans ligands changed with isosbestic points upon excitation (Figures 3 and 4) into the cis isomer and also in the case of respective complexes. The ^{1}H NMR technique has been adopted to measure the percentage composition of the irradiated solution, which supports the composition obtained from absorption spectra. The ^{1}H NMR signals of the aromatic ring protons are significantly shifted to the upper-field portion after light irradiation. The ligands and complexes show little sign of degradation upon repeated irradiation at least up to 15 cycles in each case. The structures of Cd(TaiMe)I_2·DMF (vide supra) (Figure 1) show long Cd^{II}−N(azo) distances compared to the Cd−N(imidazole) distances. Upon UV-light irradiation, the excitation may cleave the Cd−N(azo) bond easily to make a free rotatory arylazo group, which isomerizes to the cis form. The quantum yields were measured for the trans-to-cis ($\phi_{t\rightarrow c}$) photoisomerization of these compounds in MeCN upon irradiation of the UV wavelength (Table 3). The $\phi_{t\rightarrow c}$ values are significantly dependent on the nature of the substituents and counterions and the number of RaaiR′. The Me substituent at the phenylazo group (PaiR′ to TaiR′) and the Et substituent at the N1 position (1-Me to 1-Et) both reduce the $\phi_{t\rightarrow c}$ values. In general, an increase in the mass of the molecule reduces the rate of isomerization, trans to cis. In the complexes, the $\phi_{t\rightarrow c}$ values are significantly less than those of the free-ligand data. Two reasons may be considered for this decrement: (i) the presence of a coordinated CdX_2 motif heavily increases the molecular weight of the complex unit, which may severely interfere with the motion of the −N═N−Ar moiety, and (ii) the photobleaching efficiency of the halo group[28] may snatch out energy from the $\pi\pi^*$ excited state. These may cause very fast deactivation other than the photochromic route. The rotor volume has a significant influence on the isomerization rate and quantum yields.[27,29]

We have also examined the UV-light irradiation behavior of green *tcc*-Ru(PaiMe)$_2$Cl$_2$ and blue *ctc*-Ru(PaiMe)$_2$Cl$_2$[17] in MeCN. Ru^{II} complexes are silent to photoisomerization. There may be several reasons based on the structure and energy ordering of the participating functions. PaiMe is chelated to Ru^{II}, and X-ray structure determination shows that the Ru−N(azo) bond length is shorter than Ru−N(imidazole) distances. This has also prompted a charge flow of dπ(Ru) → π^*(azo), which synergistically enhances the Ru−N(azo) bond strength. This structural rigidity may resist photoisomerization. Besides, the energy transfer from $\pi\pi^*$ to the MLCT state may cause very fast bleaching.[30]

Thermal cis-to-trans isomerizations of the ligands and complexes were followed by UV−vis spectroscopy in toluene (ligands)/MeCN (complexes) at varied temperatures, 298−313 K. Eyring plots in the range 298−313 K gave a linear graph from which the activation energies were obtained (Table 4 and Figure 5). The E_a values of the free ligands are closer to those of PaiMe but lower than those of azobenzene. In the complexes, the E_a values are severely reduced, which means faster thermal cis-to-trans isomerization of the complexes. Hg-RaaiR′ halides also show higher E_a values than Cd complexes, which is also supported by the rate data.[15] The entropy of activation (ΔS^*) values are more negative in the complexes than in the free ligand. This also supports an increase in the rotor volume in the complexes.

2.5. Electronic Structure Calculation and Optical Spectra. Density functioanl theory (DFT) calculations are currently used to establish the electronic structure and spectral transitions of organic and metalloorganic compounds. In this work, DFT and time-dependent DFT (TD-DFT) calculations have been performed on $Cd(PaiMe)_2Cl_2$ (**3a**), Cd(TaiMe)I_2·DMF (**9b**), and $[Cd(PaiEt)_4](ClO_4)_2$ (**12a**) in the gas phase. The highest occupied molecular orbital (HOMO) and lowest unoccupied molecular orbital (LUMO) are abbreviated as H and L, respectively, and hence other sets of MOs. There are two sets of nearly degenerate orbitals on respective ligands in $Cd(PaiMe)_2Cl_2$. Nearly degenerate H (−5.39 eV) and H−1 (−5.44 eV) orbitals consist mainly of the 3p

(27) Nishihara, H. *Bull. Chem. Soc. Jpn.* **2004**, *77*, 407. Yutaka, T.; Mori, I.; Kurihara, M.; Mizutani, J.; Tamai, N.; Kawai, T.; Irie, M.; Nishihara, H. *Inorg. Chem.* **2002**, *41*, 7143.

(28) Zhao, X.; Chan, W.; Wong, M.; Xiao, D.; Li, Z. *Am. Lab.* **2003**, 13. Hutton, A. T.; Irving, H. M. N. H. *J. Chem. Soc., Dalton Trans.* **1982**, 2299. Zentai, G.; Partain, L.; Pavlyuchkova, R.; Proano, C.; Virshup, G.; Melekshov, L.; Zuck, A.; Breen, B. N.; Dagan, O.; Vilensky, A.; Schieber, M.; Gilboa, H.; Bennet, P.; Shah, K.; Dimitriev, Y.; Thomas, J.; Yaffe, M.; Hunter, D. *Proc. SPIE* **2003**, *5030*, June.

(29) Kepert, C. J. *Chem. Commun.* **2006**, 695. Nathan, C.; Gianneschi, M.; Masar, S., III; Mirkin, A. *Acc. Chem. Res.* **2005**, *38*, 825.

(30) Yutaka, T.; Kurihara, M.; Nishihara, H. *Mol. Cryst. Liq. Cryst.* **2000**, *343*, 193. Yutaka, T.; Mori, L.; Kurihara, M.; Mizutani, J.; Kubo, K.; Furusho, S.; Matsumura, K.; Tamai, N.; Nishihara, H. *Inorg. Chem.* **2001**, *40*, 4986.

Table 4. Rate and Activation Parameters for Cis (c) → Trans (t) Thermal Isomerization

compd	temp (K)	rate of thermal c → t convn × 10^4 (s^{-1})	E_a, kJ mol^{-1}	ΔH^*, kJ mol^{-1}	ΔS^*, J mol^{-1} K^{-1}	ΔG^*,[c] kJ mol^{-1}
PaiMe[a,d] (**1a**)	298	0.22	79.0	77.05	−77.1	100.00
	303	0.4				
	313	0.88				
	323	2.75				
TaiMe[a] (**1b**)	298	0.73	87.57	85.03	−38.84	96.60
	303	1.20				
	308	2.60				
	313	3.70				
PaiEt[a] (**2a**)	298	0.33	86.87	84.33	−47.83	98.58
	303	0.5				
	308	0.97				
	313	1.80				
TaiEt[a] (**2b**)	298	0.64	87.63	87.08	−40.20	97.06
	303	0.98				
	308	1.87				
	313	3.40				
$Cd(PaiMe)_2Cl_2$ (**3a**)	298	1.3217	26.76	24.22	−237.93	95.13
	303	1.5141				
	308	1.8007				
	313	2.2078				
$Cd(TaiMe)_2Cl_2$ (**3b**)	298	1.3617	22.80	20.26	−251.28	95.14
	303	1.5319				
	308	1.8324				
	313	2.2117				
$Cd(PaiEt)_2Cl_2$ (**4a**)	298	1.3621	24.08	21.54	−246.09	94.87
	303	1.6124				
	308	1.8406				
	313	2.1329				
$Cd(TaiEt)_2Cl_2$ (**4b**)	298	1.3928	21.35	18.81	−255.56	94.96
	303	1.6341				
	308	1.8524				
	313	2.1539				
$Cd(PaiMe)_2Br_2$ (**5a**)	298	1.6862	31.49	28.95	−219.92	94.49
	303	2.1086				
	308	2.6073				
	313	3.0894				
$Cd(TaiMe)_2Br_2$ (**5b**)	298	2.2677	25.65	23.11	−237.11	93.77
	303	2.7368				
	308	3.0947				
	313	3.7783				
$Cd(PaiEt)_2Br_2$ (**6a**)	298	1.6926	27.57	25.04	−233.13	94.51
	303	1.9939				
	308	2.4611				
	313	2.8538				
$Cd(TaiEt)_2Br_2$ (**6b**)	298	2.3629	23.64	21.10	−243.33	93.62
	303	2.9726				
	308	3.2419				
	313	3.8125				
$Cd(PaiMe)_2I_2$ (**7a**)	298	1.481	38.38	35.84	−197.97	94.84
	303	1.895				
	313	2.4236				
	323	3.1137				
$Cd(TaiMe)_2I_2$ (**7b**)	298	4.703	30.85	28.31	−213.39	91.90
	303	6.1055				
	308	7.4167				
	313	8.5429				
$Cd(PaiEt)_2I_2$ (**8a**)	298	1.557	32.58	30.03	−216.52	94.55
	303	2.22				
	308	2.582				
	313	3.25				
$Cd(TaiEt)_2I_2$ (**8b**)	298	3.663	32.1	29.56	−211.56	92.61
	303	4.594				
	308	5.292				
	313	6.906				
$Cd(PaiMe)I_2 \cdot DMF$ (**9a**)	298	2.4915	39.43	36.89	−189.95	93.50
	303	3.2877				
	308	4.4718				
	313	5.2423				
$Cd(TaiMe)I_2 \cdot DMF$ (**9b**)	298	3.6938	38.05	36.01	−189.48	92.48
	303	5.1373				
	308	6.5326				
	313	7.7931				

Table 4 (Continued)

compd	temp (K)	rate of thermal c → t convn × 10^4 (s^{-1})	E_a, kJ mol^{-1}	ΔH^*, kJ mol^{-1}	ΔS^*, J mol^{-1} K^{-1}	ΔG^*,[c] kJ mol^{-1}
$Cd(PaiEt)I_2$·DMF (**10a**)	298	2.5299	36.85	34.31	−198.36	93.42
	303	3.4926				
	308	4.3277				
	313	5.1922				
$Cd(TaiEt)I_2$·DMF (**10b**)	298	1.7629	35.93	33.38	−204.28	94.26
	303	2.5321				
	308	3.0739				
	313	3.9238				
$[Cd(PaiMe)_4](ClO_4)_2$ (**11a**)	298	2.7329	31.39	28.85	−216.07	93.24
	303	3.5639				
	308	4.3527				
	313	5.0169				
$[Cd(TaiMe)_4](ClO_4)_2$ (**11b**)	298	2.4248	22.93	20.40	−245.75	93.63
	303	2.7935				
	308	3.1578				
	313	3.8129				
$[Cd(PaiEt)_4](ClO_4)_2$ (**12a**)	298	2.8129	28.31	25.78	−226.14	93.17
	303	3.6137				
	308	4.2963				
	313	4.8732				
$[Cd(TaiEt)_4](ClO_4)_2$ (**12b**)	298	2.3647	23.14	20.60	−244.93	93.59
	303	2.9851				
	308	3.3738				
	313	3.7635				

[a] In toluene. [b] In acetonitrile. [c] At 298 K. [d] Reference 15.

Table 5. Selected List of Transition Wavelengths (Oscillator Strength) and the Major Contributions of $Cd(PaiMe)_2Cl_2$, $[Cd(PaiEt)_4](ClO_4)_2$, and $Cd(TaiMe)I_2$·DMF, Calculated in the Gas Phase by the TD-DFT Method

wavelength λ, nm (oscillator strength $f \times 10^3$)	major contribution
	$Cd(PaiMe)_2Cl_2$ (**3a**)
611.2 (0.7)	(41.5%) H → L+1, (33.9%) H → L, (37.4%) H−1 → L+1, XLCT
567.4 (7.7)	(29.2%) H−1 → L, (14%) H−3 → L+1, (16.3%) H−1 → L, XLCT
466.81 (8.1)	(22.2%) H-5 → L+1, MLCT, (19.6%) H−4 → L+1, XLCT
482.22 (4.4)	(14%) H−5 → L+1, MLCT, (28.6%) H−4 → L+1, XLCT
417.31 (19.0)	(19.5%) H−9 → L, (16.6%) H−5 → L, XLCT
363.75 (0.4)	(46%) H−7 → L+1, ILCT [π(Ph) → π^*(azo)]
341.82 (572.6)	(21%) H−6 → L+1, ILCT [π(Ph) → π^*(azo)]
328.76 (3.9)	(28.8%) H−9 → L+1, (17.4%) H−8 → L [π(Ph) → π^*(azo)]
320.12 (43.7)	(44.6%) H−11 → L [π(Ph) → π^*(azo)]
270.79 (7.6)	(36%) H → L+2, ILCT [π(Ph) → π^*(azo)]
	$Cd(TaiMe)I_2$·DMF (**9b**)
877.38 (0.8)	(49.54%) H → L, XLCT
839.36 (1.2)	(49.56%) H−1 → L, XLCT
742.55 (5.0)	(46.8%) H−2 → L, XLCT
729.13 (2.9)	(47.2%) H−3 → L, XLCT
550.01 (29.8)	(48.2%) H−4 → L, XLCT
504.86 (2.3)	(45.5%) H−5 → L, XLCT
467.56 (4.8)	(37%) H−6 → L, XLCT + [π(DMF) → π^*(azo)]
363.50 (183.3)	(30%) H−8 → L, (33%) H−10 → L, XLCT and [π(Ph) → π^*(azo)]
323.88 (0.3)	(47%) H−9 → L [π(Ph) → π^*(azo)]
289.51 (16.6)	(49.68%) H−1 → L+1, XLCT and [π(Ph) → π^*(azo)]
273.97 (18.5)	(47.29%) H−3 → L+1 [π(Ph) → π^*(azo)]
269.55 (11.7)	(35.8%) H−11 → L [π(Ph) → π^*(azo)]
	$[Cd(PaiEt)_4](ClO_4)_2$ (**12a**)
464.12 (27.3)	(12%) H−2 → L+1, (11%) H−5 → L, $\pi \rightarrow \pi^*$
407.64 (16.6)	(19%) H → L, (15%) H−1 → L+4, (15%) H−1 → L+1, $\pi \rightarrow \pi^*$
398.71 (0.9)	(23%) H−1 → L+1, (28%) H−3 → L+1, $\pi \rightarrow \pi^*$
368.90 (49.5)	(18%) H−4 → L+1, (15%) H−3 → L+2, $\pi \rightarrow \pi^*$ and n → π^*
353.43 (16.9)	(32%) H−5 → L+1, (32%) H−7 → L, (40%) H−6 → L+3, $\pi \rightarrow \pi^*$, n → π^*
347.31 (150.5)	(19%) H−8 → L+1, (27%) H−8 → L, $\pi \rightarrow \pi^*$, n → π^*
330.01 (3.7)	(19%) H−6 → L, (32%) H−8 → L+3, $\pi \rightarrow \pi^*$, n → π^*
312.22 (3.6)	(40%) H−6 → L+2, (25%) H−10 → L+2, $\pi \rightarrow \pi^*$, n → π^*

orbitals of the Cl ligands (Figure 6) bonded to the Cd ion. The occupied MOs other than H, such as H−1 to H−5, are bonding orbitals comprised of mixtures of 3p(Cl), n(imidazole), and 4d(Cd). Further below (H−6, H−7, etc.) are π orbitals of the (phenylazo)imidazole ligands. L (LUMO; −2.75 eV) and L+1 (LUMO+1; −2.69 eV) are nearly degenerate π^* orbitals of the (phenylazo)imidazoles. In the case of $Cd(TaiMe)I_2$·DMF, H (−5.17 eV) and H−1 (−5.25

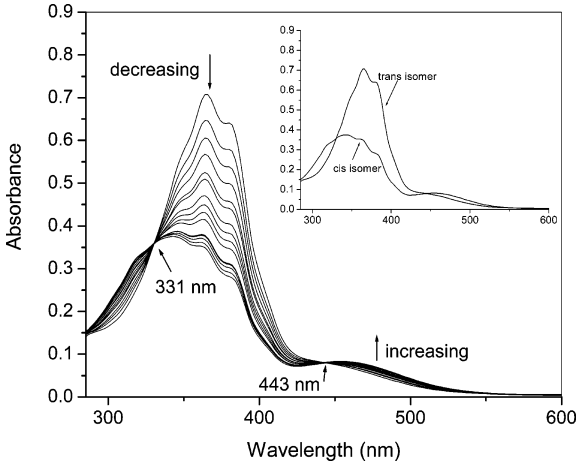

Figure 4. Spectral changes of TaiMe in toluene upon repeated irradiation at 365 nm at 3 min intervals at 25 °C. The inset shows spectra of the cis and trans isomers of TaiMe.

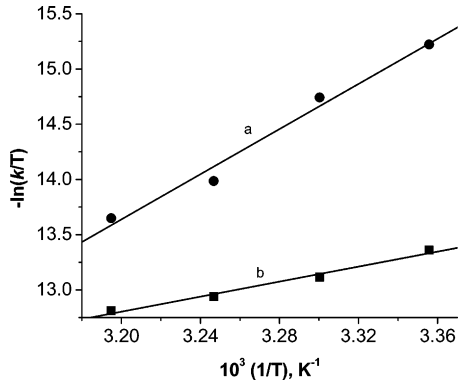

Figure 5. Eyring plots of thermal cis-to-trans isomerization of (a) TaiMe and (b) [Cd(TaiMe)I_2].

eV) are also closely spaced and consist mainly of the 5p orbitals (Figure 6) of the I ligands bonded to the Cd ion. The lower-energy orbitals (H−2 to H−6) are bonding orbitals comprised of mixtures of 5p(I), n(imidazole), and 4d(Cd). Further below, the orbitals H−7, H−8, etc., are localized on the *p*-tolyl moiety of TaiMe. The LUMO (L) is a π^* orbital delocalized over the entire (phenylazo)imidazole moiety, while L+1 and L+2 are also π^* orbitals but rather are localized on the phenyl and imidazole groups, respectively. In [Cd(PaiEt)$_4$](ClO_4)$_2$, four PaiEt ligands coordinate to a Cd ion in a tetrahedral geometry. Each two of the four ligands are crystallographically equivalent. The cationic complex excluding the counteranions was subjected to the calculation. Metal-centered orbitals contribute little to the frontier orbitals (Figure 6), which are therefore dominated by ligand orbitals. Then, the orbitals on the ligands are perturbed by mutual interchromophoric interactions within the complex. As a consequence, a significant mixing of n and π orbitals is recognized. The first three occupied orbitals, H (−10.97 eV), H−1 (−10.99 eV), and H−2 (−11.05 eV), are energetically close to each other, and all of these MOs are mainly constituted of ligand orbitals. The L (−7.40 eV) and L+1 (−7.40 eV) orbitals are degenerate as are the L+2 (−7.18 eV) and L+3 (−7.16 eV) levels. These MOs are constituted of ligand π^* levels.

To gain detailed insight into the charge transitions, TD-DFT calculations were performed on the above complexes in the gas phase (Table 5). The transitions at longer wavelength are coming from X(Cl or I) → π^*(azoimine) charge-transfer transitions (abbreviated in Table 5 as XLCT) along with a series of Cd-to-(phenylazo)imidazole charge-transfer transitions (mainly low intensities). They are predicted in the range between 880 and 370 nm. Strong $\pi-\pi^*$ transitions (H−8/H−7 to L+1 with charge-transfer character are expected around 350−360 nm). The calculation of Cd(PaiMe)$_2$$Cl_2$ shows a series of Cl/Cd-to-(phenylazo)imidazole charge-transfer transitions (mainly from H or H−6 to L and L+1 with low intensities) predicted in the range between 610 and 360 nm. Strong $\pi-\pi^*$ transitions (H−7 to L and H−6 to L+1) are expected at around 340 nm. These are defined as intraligand charge-transfer transitions. Optical transitions are predicted in the range <470 nm. Among them, transitions that have a large oscillator strength (>0.1) are as follows: 348 nm [H−1 (π) to L+3 (π^*)]; 347 nm [H−8 (n/π) to L+1 (π^*)]; 327 nm [H−11 (n) to L+2 (π^*)]; 325 nm [H−10 (n) to L+3 (π^*)].

An energy correlation diagram (Figure 7) of MOs shows a decrease in the energies of the respective unoccupied orbitals in the order of Cd(PaiMe)$_2$$Cl_2$ > Cd(PaiMe)I_2·DMF <<< [Cd(PaiEt)$_4$](ClO_4)$_2$. The occupied MOs show a small increment in energy on going from Cd(PaiMe)$_2$$Cl_2$ to Cd(PaiMe)I_2·DMF, while a huge fall in energy is observed to [Cd(PaiEt)$_4$](ClO_4)$_2$. Besides, the energy difference ($\Delta E = E_{LUMO} - E_{HOMO}$) between HOMO and LUMO follows the ordering Cd(PaiMe)I_2·DMF (2.03 eV) < Cd(PaiMe)$_2$$Cl_2$ (2.64 eV) < [Cd(PaiEt)$_4$](ClO_4)$_2$ (3.57 eV). The plots of ΔE versus rates of isomerization and quantum yields are linearly related (Figure 8). This implies the direct correlation between the photophysical process and the activation energy barrier.

In the photochromic process, UV-light irradiation is mandatory for the molecule in solution for a fixed time, which will enforce isomerization from the more stable trans isomer to the cis isomer. Irradiation in the UV region (360−395 nm) may be responsible for the $\pi \rightarrow \pi^*$ transition. The MLCT or XLCT (X = Cl or I) is a lower energetic transition, which is capable of charge transfer to azoimidazole but its energy is insufficient to perform a physical process like isomerization. Conversely, the metalated ligand may perform a charge transition in a secondary (MLCT or XLCT) process, which is responsible for deactivation of excited-state species and reduces the rate of the trans → cis change and quantum yields. This is indeed observed (Table 3).

3. Experimental Section

3.1. Materials. $CdCl_2$, $CdBr_2$, and CdI_2 were obtained from Loba Chemicals, Bombay, India. 1-Alkyl-2-(arylazo)imidazoles were synthesized by a reported procedure.[15] All other chemicals and solvents were reagent-grade as received.

3.2. Physical Measurements. Microanalytical data (C, H, and N) were collected on a Perkin-Elmer 2400 CHNS/O elemental analyzer. Spectroscopic data were obtained using the following instruments: UV−vis spectra from a Perkin-Elmer Lambda 25 spectrophotometer; IR spectra (KBr disk, 4000−200 cm^{-1}) from a

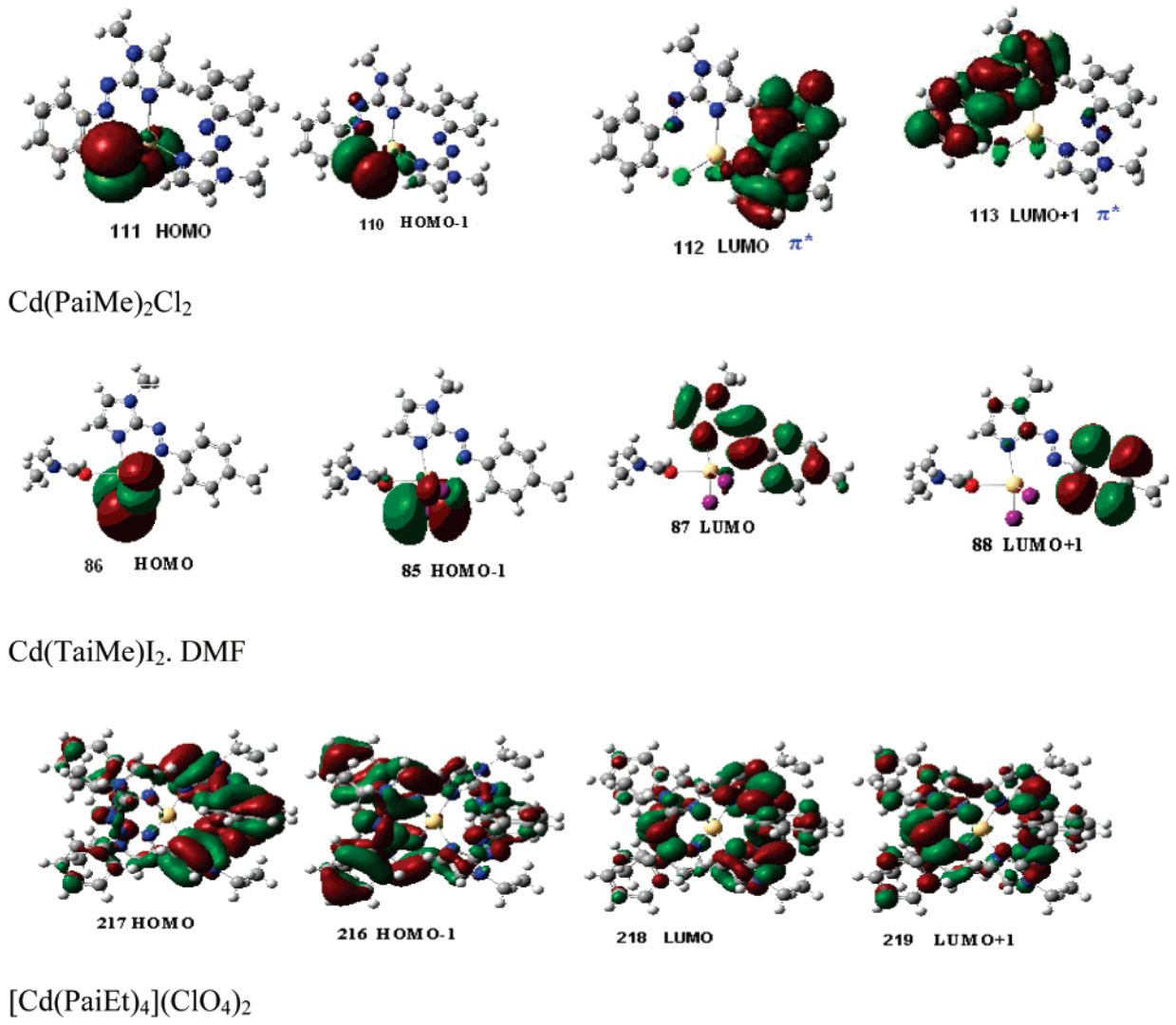

Figure 6. Some MO pictures (HOMO, HOMO−1, LUMO, and LUMO+1) of $Cd(PaiMe)_2Cl_2$, $Cd(PaiMe)I_2$·DMF, and $[Cd(PaiEt)_4](ClO_4)_2$.

Perkin-Elmer RX-1 FTIR spectrophotometer; photoexcitation carried out using a Perkin-Elmer LS-55 spectrofluorimeter; ^{1}H NMR spectra from a Bruker (AC) 300 MHz FTNMR spectrometer.

3.3. Synthesis of $[Cd(TaiMe)_2I_2]$ (7b). TaiMe (140 mg, 0.7 mmol) in MeOH (20 mL) was added dropwise to an acetonitrile solution (5 mL) of CdI_2 (125 mg., 0.34 mmol), which was refluxed for 2 h. An orange-yellow precipitate appeared. The precipitate was collected by filtration, washed with cold MeOH, and dried over $CaCl_2$ in vacuo. The yield was 168 mg (64%). Other complexes were prepared under identical conditions, and the yield varied in the range 60−70%.

Microanalytical data. Calcd for $C_{20}H_{20}N_8Br_2Cd$ (**5a**): C, 37.24; H, 3.10; N, 17.38. Found: C, 37.15; H, 3.00; N, 17.46. Calcd for $C_{22}H_{24}N_8Br_2Cd$ (**5b**): C, 39.26; H, 3.57; N, 16.66. Found: C, 39.12; H, 3.60; N, 16.49. Calcd for $C_{22}H_{24}N_8Br_2Cd$ (**6a**): C, 39.26; H, 3.57; N, 16.66. Found: C, 39.21; H, 3.52; N, 16.59. Calcd for $C_{24}H_{28}N_8Br_2Cd$ (**6b**): C, 41.12; H, 4.00; N, 15.99. Found: C, 41.20; H, 4.10; N, 16.10. Calcd for $C_{20}H_{20}N_8I_2Cd$ (**7a**): C, 32.50; H, 2.71; N, 15.17. Found: C, 32.40; H, 2.65; N, 15.29. Calcd for $C_{22}H_{24}N_8I_2$-Cd (**7b**): C, 34.45; H, 3.13; N, 14.61. Found: C, 34.52; H, 3.10; N, 14.70. Calcd for $C_{22}H_{24}N_8I_2Cd$ (**8a**): C, 34.45; H, 3.13; N, 14.61. Found: C, 34.56; H, 3.18; N, 14.58. Calcd for $C_{24}H_{28}N_8I_2Cd$ (**8b**): C, 36.25; H, 3.52; N, 14.10. Found: C, 36.32; H, 3.60; N, 14.20. Calcd for $C_{13}H_{17}N_5$ OI_2Cd (**9a**): C, 24.94; H, 2.72; N, 11.19. Found: C, 25.00; H, 2.80; N, 11.10. Calcd for $C_{14}H_{19}N_5OI_2Cd$ (**9b**): C, 26.27; H, 2.97; N, 10.95. Found: C, 26.35; H, 3.05; N, 11.04. Calcd for $C_{14}H_{19}N_5OI_2Cd$ (**10a**): C, 26.27; H, 2.97; N, 10.95. Found: C, 26.39; H, 3.00; N, 11.00. Calcd for $C_{15}H_{21}N_5OI_2Cd$ (**10b**): C, 27.55; H, 3.21; N, 10.71. Found: C, 27.60; H, 3.25; N, 10.80.

3.4. X-ray Diffraction Study. The crystallographic data are shown in Table 6. A suitable single crystal of the complex (0.30 × 0.25 × 0.20 mm) was mounted on a CrysAlis CCD, Oxford Diffraction Ltd. diffractometer equipped with graphite-monochromated Mo Kα (λ = 0.710 73 Å) radiation. The unit cell parameters and crystal-orientation matrices were determined by least-squares refinements of all reflections. The intensity data were corrected for Lorentz and polarization effects, and an empirical absorption correction was also employed using the *SAINT* program.[31] Data were collected by applying the condition $I > 2\sigma(I)$. All of these structures were solved by direct methods followed by successive Fourier and difference Fourier syntheses. Full-matrix least-squares refinements on F^2 were carried out using *SHELXL-97* with anisotropic displacement parameters for all non-H atoms. H atoms were constrained to ride on the respective C or N atoms with isotropic displacement parameters equal to 1.2 times the equivalent isotropic displacement of their parent atom in all cases. Complex

(31) Bruker. *SMART and SAINT*; Bruker AXS Inc.: Madison, WI, 1998.

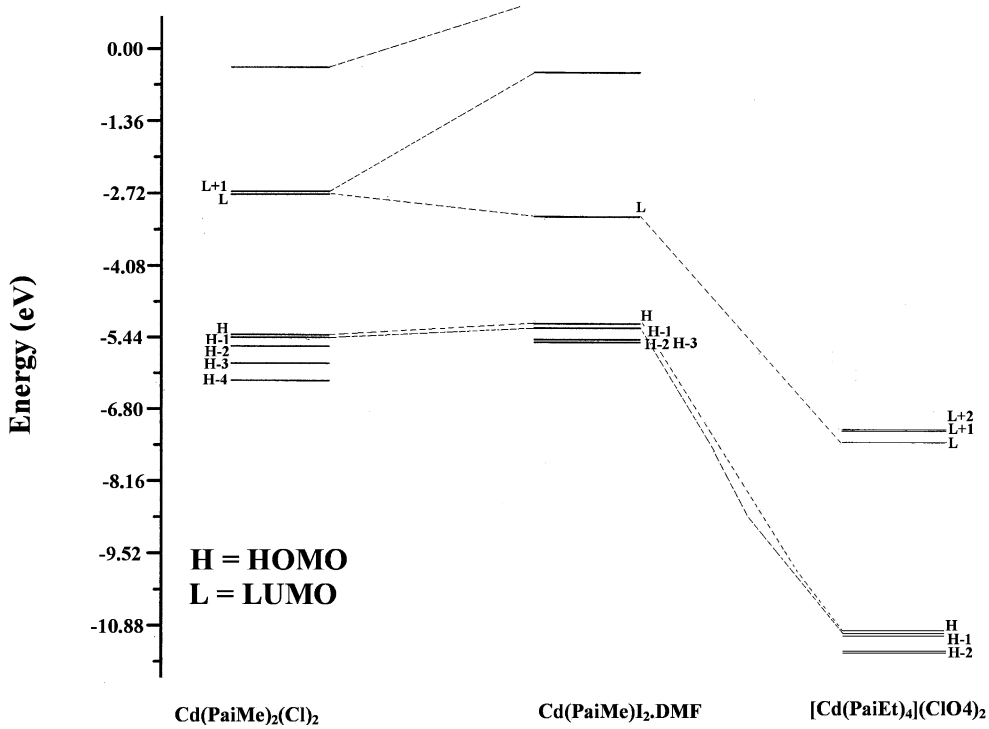

Figure 7. Energy correlation diagram for MOs of $Cd(PaiMe)_2Cl_2$, $Cd(TaiMe)I_2$·DMF, and $[Cd(PaiEt)_4](ClO_4)_2$.

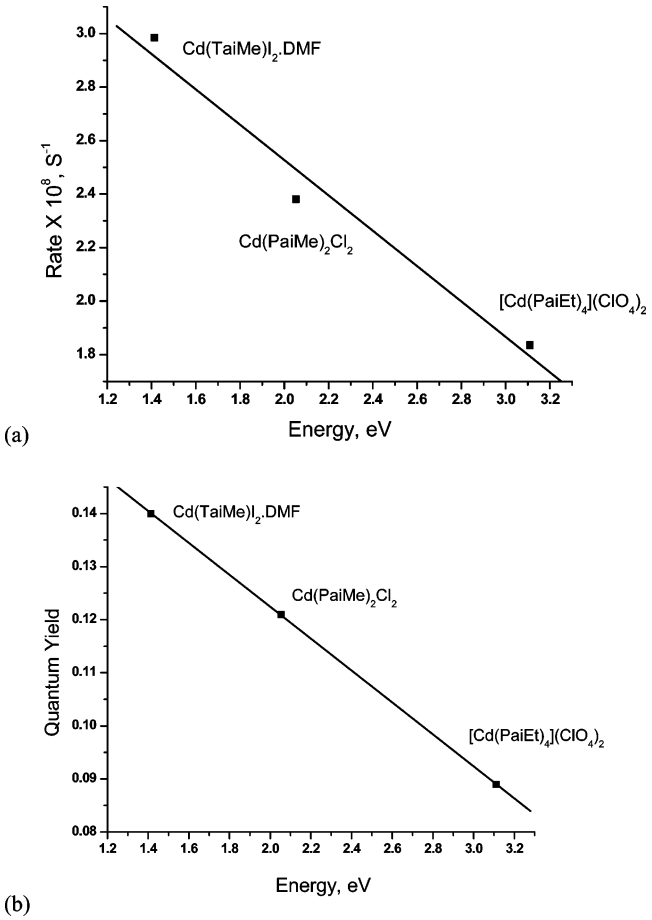

Figure 8. Correlation between ΔE ($=E_{LUMO} - E_{HOMO}$) and (a) the rates of photoisomerization and (b) the quantum yields.

neutral atom scattering factors were used throughout for all cases. All calculations were carried out using *SHELXS 97*,[32] *SHELXL97*,[33] *PLATON 99*,[34] and *ORTEP-3*[35] programs.

Table 6. Summarized Crystallographic Data for **9b**

compound	$[Cd(TaiMe)I_2(C_3H_6NO)]$ (**9b**)
empirical formula	$C_{14}H_{18}CdI_2N_5O$
fw	638.53
T (K)	293(2)
cryst syst	triclinic
space group	$P\bar{1}$
cryst size (mm^3)	0.30 × 0.25 × 0.20
a (Å)	8.244(2)
b (Å)	10.408(3)
c (Å)	13.512(4)
α (deg)	83.63(3)
β (deg)	86.59(3)
γ (deg)	65.35(3)
V ($Å^3$)	1047.0(5)
Z	2
λ (Å)	0.710 73
μ(Mo Kα) (mm^{-1})	4.000
θ range (deg)	2.96−25.00
hkl range	$-9 < h < 9$; $-12 < k < 12$; $-16 < l < 16$
D_{calc} (mg m^{-3})	2.025
refined param	208
total reflns	9518
unique reflns	3626
R1[a] [$I > 2\sigma(I)$]	0.0367
wR2[b]	0.0897
GOF	1.038

[a] $R1 = \sum||F_o| - |F_c||\sum|F_o|$. [b] $wR2 = [\sum w(F_o^2 - F_c^2)^2/\sum w(F_o^2)^2]^{1/2}$, $w = 1/[\sigma^2(F_o)^2 + (0.0415P)^2 + (1.5065P)]$ where $P = ((F_o^2 + 2F_c^2)/3$.

3.5. Photometric Measurements. Absorption spectra were taken with a Perkin-Elmer Lambda 25 UV−vis spectrophotometer in a 1 × 1 cm quartz optical cell maintained at 25 °C with a Peltier thermostat. The light source of a Perkin-Elmer LS 55 spectrofluorimeter was used as an excitation light, with a slit width of 10 nm.

(32) Sheldrick, G. M. *SHELXS 97, Program for the Solution of Crystal Structure*; University of Göttingen: Göttingen, Germany, 1997.
(33) Sheldrick, G. M. *SHELXL 97, Program for the Solution of Crystal Structure*; University of Göttingen: Göttingen, Germany, 1997.
(34) Spek, A. L. *PLATON, Molecular Geometry Program*; University of Utrecht: Utrecht, The Netherlands, 1999.

An optical filter was used to cut off overtones when necessary. The absorption spectra of the cis isomers were obtained by extrapolation of the absorption spectra of a cis-rich mixture for which the composition is known from ^{1}H NMR integration. Quantum yields (ϕ) were obtained by measuring the initial trans-to-cis isomerization rates (ν) in a well-stirred solution within the above instrument using the equation

$$\nu = (\phi I_0/V)(1 - 10^{-\mathrm{Abs}})$$

where I_0 is the photon flux at the front of the cell, V is the volume of the solution, and Abs is the initial absorbance at the irradiation wavelength. The value of I_0 was obtained by using azobenzene ($\phi = 0.11$ for $\pi\pi^*$ excitation[26]) under the same irradiation conditions.

The thermal cis-to-trans isomerization rates were obtained by monitoring absorption changes intermittently for a cis-rich solution kept in the dark at constant temperatures (T) in the range from 298 to 313 K. The activation energy (E_a) and the frequency factor (A) were obtained from the Arrhenius plot

$$\ln k = \ln A - E_a/RT$$

where k is the measured rate constant, R is the gas constant, and T is the temperature. The values of the activation free energy (ΔG^*) and the activation entropy (ΔS^*) were obtained through the relationships

$$\Delta G^* = E_a - RT - T\Delta S^* \quad \text{and} \quad \Delta S^* = \ln A - 1 - \ln(k_B T/h)/R$$

where k_B and h are Boltzmann's and Plank's constants, respectively.

3.6. DFT Calculations. DFT calculations were carried out using X-ray crystallographic parameters of $Cd(PaiMe)_2Cl_2$ (**3a**), $Cd(PaiEt)_4](ClO_4)_2$ (**12a**), and Cd(TaiMe)I_2·DMF (**9b**). A *Gaussian 03w* package[36] was run on a personal computer. The functional B3LYP[37] and basis set LanL2DZ[38] were chosen for the calculations. The electronic spectrum was calculated with the TD-DFT method. For nonmetallic atoms, diffuse and polarization functions were used. Natural bond order (NBO) calculations were performed with the NBO code included in *Gaussian 03*.

4. Conclusion

Cadmium(II) halide complexes of 1-alkyl-2-(arylazo)-imidazoles are described. One of the complexes has been characterized by a single-crystal X-ray structure study. Photochromism of the complexes is examined by UV-light irradiation in a MeCN solution, and the results are compared with free-ligand data. Quantum yields of trans-to-cis isomerization are determined in toluene for ligands and in MeCN for complexes. The cis-to-trans isomerization is a thermally driven process. The activation energy (E_a) of the cis-to-trans isomerization has been calculated. The slow rate of isomerization in complexes may be due to a higher rotor volume than that of free ligands.

Acknowledgment. Financial support from the Council of Scientific and Industrial Research (CSIR), New Delhi, India, is gratefully acknowledged. We thank the National Single-Crystal Facility Centre, IIT, Bombay, Mumbai, India, for help regarding X-ray crystallographic data collection.

Supporting Information Available: X-ray crystallographic data for the structures in CIF format. This material is available free of charge via the Internet at http://pubs.acs.org. This file has also been deposited with the Cambridge Crystallographic Data Centre as CCDC 635225. Copies of this information may be obtained free of charge from the Director, CCDC, 12 Union Road, Cambridge CB2 1EZ, U.K. (e-mail: deposit@ccdc.cam.ac.uk or www:htpp://www.ccdc.cam.ac.uk).

IC7012073

(35) Farrugia, L. J. ORTEP-3 for windows. *J. Appl. Crystallogr*. **1997**, *30*, 565.

(36) Frisch, M. J.; Trucks, G. W.; Schlegel, H. B.; Scuseria, G. E.; Robb, M. A.; Cheeseman, J. R.; Montgomery, J. A., Jr.; Vreven, T.; Kudin, K. N.; Burant, J. C.; Millam, J. M.; Iyengar, S. S.; Tomasi, J.; Barone, V.; Mennucci, B.; Cossi, M.; Scalmani, G.; Rega, N.; Petersson, G. A.; Nakatsuji, H.; Hada, M.; Ehara, M.; Toyota, K.; Fukuda, R.; Hasegawa, J.; Ishida, M.; Nakajima, T.; Honda, Y.; Kitao, O.; Nakai, H.; Klene, M.; Li, X.; Knox, J. E.; Hratchian, H. P.; Cross, J. B.; Bakken, V.; Adamo, C.; Jaramillo, J.; Gomperts, R.; Stratmann, R. E.; Yazyev, O.; Austin, A. J.; Cammi, R.; Pomelli, C.; Ochterski, J. W.; Ayala, P. Y.; Morokuma, K.; Voth, G. A.; Salvador, P.; Dannenberg, J. J.; Zakrzewski, V. G.; Dapprich, S.; Daniels, A. D.; Strain, M. C.; Farkas, O.; Malick, D. K.; Rabuck, A. D.; Raghavachari, K.; Foresman, J. B.; Ortiz, J. V.; Cui, Q.; Baboul, A. G.; Clifford, S.; Cioslowski, J.; Stefanov, B. B.; Liu, G.; Liashenko, A.; Piskorz, P.; Komaromi, I.; Martin, R. L.; Fox, D. J.; Keith, T.; Al-Laham, M. A.; Peng, C. Y.; Nanayakkara, A.; Challacombe, M.; Gill, P. M. W.; Johnson, B.; Chen, W.; Wong, M. W.; Gonzalez, C.; Pople, J. A. *Gaussian 03*, revision C.02; Gaussian, Inc.: Wallingford, CT, 2004.

(37) B3LYP: Becke, A. D. *J. Chem. Phys*. **1993**, *98*, 5648.

(38) LanL2DZ: (a) Hay, P. J.; Wadt, W. R. *J. Chem. Phys*. **1985**, *82*, 270. (b) Wadt, W. R.; Hay, P. J. *J. Chem. Phys.* **1985**, *82*, 284. (c) Hay, P. J.; Wadt, W. R. *J. Chem. Phys.* **1985**, *82*, 299.